An RNA-Binding Peptide from Bovine Immunodeficiency Virus Tat Protein Recognizes an Unusual RNA Structure†

Lily Chen and Alan D. Frankel*

Department of Biochemistry and Biophysics and Gladstone Institute of Virology and Immunology, University of California, P.O. Box 419100, San Francisco, California 94141

Received September 8, 1993; Revised Manuscript Received December 7, 1993®

ABSTRACT: The human immunodeficiency virus (HIV) Tat protein binds specifically to an RNA hairpin, TAR, located at the 5′ end of its mRNA. Tat uses a single arginine residue within a short region of basic amino acids to recognize a bulge region in TAR. Here we show that a 17 amino acid arginine-rich peptide from the bovine immunodeficiency virus (BIV) Tat protein also binds to an RNA hairpin at the 5′ end of its mRNA (BIV TAR), but recognizes different structural features of the RNA. Mutagenesis, RNase mapping, and chemical interference experiments indicate that bulge and stem regions of BIV TAR are recognized simultaneously by the BIV peptide and that the RNA adopts an unusual structure. BIV Tat binds to its TAR site with high affinity and specificity and, unlike HIV Tat, does not appear to use cellular proteins to stabilize RNA binding in vivo. Thus, two related viral activators have evolved rather distinct ways to recognize their RNA targets.

The folding of an RNA molecule determines the precise arrangement of its functional groups and thus plays an important role in sequence-specific RNA–protein recognition. The cocrystal structures of two tRNA synthetase–tRNA complexes have shown not only that the RNAs share structural complementarity with their cognate proteins but that they change conformation upon binding, repositioning groups on the bases and backbone for specific interactions (Rould et al., 1989, 1991; Ruff et al., 1991; Cavarelli et al., 1993). Similarly, RNA-binding studies using model peptides from the human immunodeficiency virus (HIV) Tat and Rev proteins have shown that tertiary features of the RNA and conformational changes are important for specific recognition (Frankel, 1992; Tan et al., 1993).

Tat and Rev are members of a class of RNA-binding proteins, including bacterial antiterminators and ribosomal proteins, that contain an arginine-rich motif approximately 10–20 amino acids in length (Lazinski et al., 1989). Tat binds to TAR RNA (the trans-acting response element), and Rev binds to RRE RNA (the Rev response element). In each case, a short peptide containing just the arginine-rich domain (9 amino acids from Tat and 17 amino acids from Rev) binds to its RNA site with specificity similar to that of the intact protein (Weeks et al., 1990; Calnan et al., 1991a; Kjems et al., 1992). In Tat, a single arginine is responsible for specific recognition of a bulge region in TAR (Calnan et al., 1991b; Puglisi et al., 1992; Tao & Frankel, 1992), with surrounding basic amino acids needed to raise the RNA-binding affinity and enhance the arginine-binding specificity (Tao & Frankel, 1993). The arginine-rich domain of Tat appears to be unstructured, even in the context of the intact protein (Calnan et al., 1991a,b). In contrast, the arginine-rich domain of Rev binds specifically to the RRE only when in an α-helical conformation and appears to use six amino acids (four arginines, one threonine, and one asparagine) for specific recognition (Tan et al., 1993). Thus, while it may be convenient to classify Tat and Rev together as members of the arginine-rich class of RNA-binding proteins, it seems clear that the structural motifs used for recognition are quite distinct.

Because Tat and Rev recognize their RNA-binding sites in such different ways, studies of other arginine-rich domains are likely to reveal different features of RNA–protein recognition and to provide interesting comparisons. In this study, we examine the RNA-binding properties of a peptide from the bovine immunodeficiency virus (BIV) Tat protein. BIV is a recently characterized lentivirus, related to the human and simian viruses (HIV and SIV), that causes persistent lymphocytosis, lymphadenopathy, and central nervous system lesions in infected cows (Gonda, 1992). The BIV genome contains the essential retroviral structural genes, *gag*, *pol*, and *env*, flanked by the LTR on the 5′ and 3′ termini in addition to at least five accessory genes analogous to *tat*, *rev*, *vif*, *vpr*, and *vpu* of HIV (Gonda, 1992). BIV Tat is encoded by two exons and shares sequence similarity to the HIV and SIV proteins (Garvey et al., 1990). A Tat-like factor from BIV-infected cells has been shown to activate the viral LTR (Pallansch et al., 1992), and BIV Tat cDNA clones have been shown to activate both the BIV and HIV promoters (Liu et al., 1992). Here we show that, as with HIV Tat, the arginine-rich region of BIV Tat recognizes an RNA target (BIV TAR) located at the 5′ end of the viral mRNAs. However, both in vitro and in vivo results suggest that while certain recognition features are shared by the BIV and HIV Tat proteins, the TAR RNA structures formed by the two viruses are rather distinct and their dependence on host RNA-binding factors appears to be different. The results emphasize that a simple "recognition code" is unlikely to exist for RNA–protein recognition and that, as for DNA–protein recognition, structural comparisons of related and unrelated motifs (both protein and RNA) will be needed to more completely define the interactions that contribute to sequence-specific binding.

† Supported by NIH Grant AI29135, by Sterling Drug Co., and by NIH Fellowship AI08591 (L.C.).

* Address correspondence to this author at Gladstone Institute/Biochemistry and Biophysics, UCSF, P.O. Box 419100, San Francisco, CA 94141.

® Abstract published in *Advance ACS Abstracts,* February 1, 1994.

0006-2960/94/0433-2708$04.50/0

MATERIALS AND METHODS

Peptide Synthesis, Purification, and Analysis. BIV Tat peptides were synthesized on a Milligen/Biosearch Model 9600 peptide synthesizer as described (Tan et al., 1993) or on an Applied Biosystems Model 432A peptide synthesizer. On the Applied Biosystems synthesizer, the BIV peptide was synthesized using Fmoc chemistry and standard Applied Biosystems resin (25 μmol) and protecting groups. The N-terminus was acetylated using acetic acid (75 μmol) with HBTU activation. Following cleavage and deprotection in the presence of reagent R, peptides were purified on a C_4 reverse-phase HPLC column (Vydac) using an acetonitrile gradient of 0.2%/min in 0.1% trifluoroacetic acid. Absorption spectra were used to calculate peptide concentration using known peptides as standards. Purity and concentrations were confirmed by native gel electrophoresis (20% polyacrylamide in 30 mM sodium acetate, pH 4.5) in which peptides were visualized by Coomassie blue staining. Peptide molecular weights were confirmed by electrospray mass spectrometry (D. King, University of California, Berkeley).

RNA Synthesis and Purification. Wild-type and mutant BIV TAR RNAs were transcribed in vitro by T7 RNA polymerase using synthetic oligonucleotide templates (Milligan & Uhlenbeck, 1989). All RNAs contained GG at the 5′ end, which increases the efficiency of transcription, and CC at the 3′ end to base pair with the G's. For randomly labeled RNAs, [α-^{32}P]CTP (NEN, 3000 Ci/mmol) was included in the transcription reaction. To label RNAs at their 5′ ends, dephosphorylated RNAs were incubated with [γ-^{32}P]ATP (NEN, 6000 Ci/mmol) and T4 polynucleotide kinase. RNAs were purified on 20% polyacrylamide/8 M urea gels, eluted from the gels in 0.6 M NaOAc, pH 6.0, 1 mM EDTA, and 0.01% SDS, and ethanol precipitated twice. Purified RNA was resuspended in sterile deionized water. The concentrations of radiolabeled RNAs were determined from the specific activity of [^{32}P]CTP incorporated into the transcripts. Unlabeled RNAs were quantitated by spectrophotometry. RNAs were renatured by incubating in renaturation buffer (10 mM Tris-HCl, pH 7.5, and 70 mM NaCl) for 2 min at 85 °C followed by slow cooling to room temperature.

RNA-Binding Gel Shift Assays. Gel shift assays were performed at 4 °C. Peptide and RNA typically were incubated together for 30 min on ice in 10-μL binding reaction mixtures containing 10 mM Tris-HCl, pH 7.5, 70 mM NaCl, 0.2 mM EDTA, 5% glycerol, and 25 μg/mL yeast tRNA. To determine relative binding affinities, 0.1–0.25 nM radiolabeled BIV TAR RNA (or TAR mutants) was titrated with peptide. To measure apparent binding constants directly and to determine binding stoichiometries, some reactions were performed in the absence of competitor RNA with 0.05–2.5 nM labeled BIV TAR RNA. Varying the time of the binding reaction indicated that equilibrium had been reached within 1 min. Peptide–RNA complexes were resolved on 10% polyacrylamide/0.5× TBE gels that had been prerun for 1 h and allowed to cool to 4 °C. Gels were electrophoresed at 200 V for 2.5 h at 4 °C, dried, and autoradiographed.

Construction of Plasmids and CAT Assays. The BIV TAR reporter plasmid was constructed by cloning synthetic oligonucleotide cassettes into the HIV LTR of pHIV-CAT as described (Tao & Frankel, 1993). HIV Tat–BIV peptide hybrids were constructed by cloning a BIV peptide-encoding cassette into the *tat* gene of pSV2tat72 after Tat amino acid 48 (Tan et al., 1993). Mutations were confirmed by dideoxynucleotide sequencing. Reporter plasmids (50 ng) and HIV Tat or Tat–BIV peptide fusion plasmids (50–200 ng) were transfected into HeLa or mouse LTk$^-$ cells, and CAT activity was assayed after 48 h and quantitated as described (Calnan et al., 1991a). Total amounts of plasmid DNA were adjusted to 1 μg of with nonspecific pBR322 DNA.

RNase Mapping and Peptide Footprints. Approximately 250 ng (10^6 cpm) of renatured 5′-end-labeled RNA was resuspended in 100 μL of structure probing buffer (10 mM Tris-HCl, pH 7.0, 10 mM $MgCl_2$, 100 mM NaCl, and 20 μg/mL yeast tRNA). The sample was divided into four aliquots, and each was incubated with 25 μL of diluted BIV peptide or H_2O at 0 °C for 30 min. Each reaction mixture was further divided into six aliquots and treated with RNases T1 (0.03 unit; Pharmacia), PhyM (0.06 unit; Pharmacia), CV (0.002 unit; Pharmacia), CL3 (0.004 unit; Boehringer), A (0.05 munit; Boehringer), or T2 (0.12 unit; BRL) at 0 °C for 15–30 min. Final peptide concentrations were 5 nM, 25 nM, and 125 nM, and the final TAR RNA concentration was ~110 nM. Formamide (10 μL) was added to each reaction mixture and samples were electrophoresed on 17% polyacrylamide/8 M urea sequencing gels. No RNase digestion was observed immediately after formamide addition, and longer incubations in the presence of formamide showed decreased rates of reaction and digestion patterns identical to those in the absence of formamide, indicating that exposure to formamide during the time course of these experiments did not alter the RNA structure. An alkaline hydrolysis ladder and RNase sequencing reactions were included on the gels as markers.

Chemical Modification Interference. Approximately 250–500 ng (2×10^6 cpm) of 5′-end-labeled BIV TAR RNA was mixed with 10 μg of unlabeled RNA and modified at less than one site per molecule with dimethyl pyrocarbonate (DMPC; Sigma), diethyl pyrocarbonate (DEPC; Sigma), hydrazine (HZ; Sigma), or dimethyl sulfate (DMS; Aldrich) essentially as described (Peattie, 1979) or with ethylnitrosourea (ENU; Sigma) according to Calnan et al. (1991b). Modification reactions were carried out under denaturing RNA conditions. RNA was ethanol precipitated twice and applied onto a BIV_{65-81} peptide affinity column. The peptide column was prepared as described by Tan and Frankel (1992): 0.5 mg of a BIV peptide containing an N-terminal cysteine was coupled to 0.5 mL of (ω-aminohexyl)agarose resin (Sigma) via the cysteine thiol using a maleimidosuccinimide ester bifunctional cross-linker (Pierce). The coupling reaction was performed in an anaerobic chamber for 2 h followed by incubation at 4 °C overnight. A mixture of 5 μg each of modified BIV TAR and HIV TAR containing a deletion of the 3-nucleotide bulge (as a nonspecific RNA control) was applied to the peptide affinity column, and RNAs were eluted at 4 °C with an NaCl gradient. The HIV TAR bulge deletion and BIV TAR RNAs modified at positions that interfered with binding eluted at 430 mM NaCl, whereas BIV TAR bound specifically to the column eluted at 900 mM NaCl. Eluted RNAs were ethanol precipitated, cleaved at the modified positions by aniline (Fluka), and analyzed on 17–20% polyacrylamide/8 M urea gels. The cleavage patterns of specifically bound fractions were compared to cleaved modified RNAs that had not been run on the column (total RNA) to identify modified positions that interfered with binding. Alkaline hydrolysis ladders and RNase sequencing reactions were included as markers.

RESULTS

An Arginine-Rich Peptide from BIV Tat Binds Specifically to BIV TAR. HIV Tat contains a 9 amino acid arginine-rich

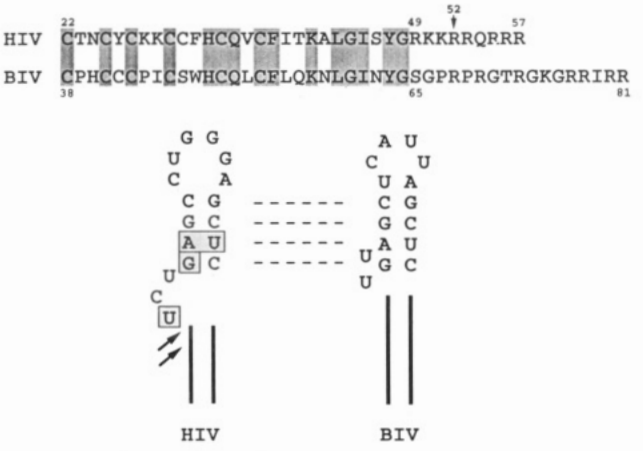

FIGURE 1: Comparisons of HIV-1 and BIV Tat proteins and TAR RNA sites. Tat protein sequences are aligned by their cysteine-rich and conserved core domains (top). Conserved residues are highlighted. Arginine 52 in HIV Tat (arrow) mediates specific recognition of HIV TAR. The basic region of BIV Tat spans residues 65–81. The two RNA hairpins shown (bottom) are located near the 5′ ends of their respective mRNAs. In HIV TAR, the boxed nucleotides and two phosphates indicated by arrows are important for Tat binding. In BIV TAR, two bulge uridines and a sequence similar to the upper stem of HIV TAR (dashed lines) are observed.

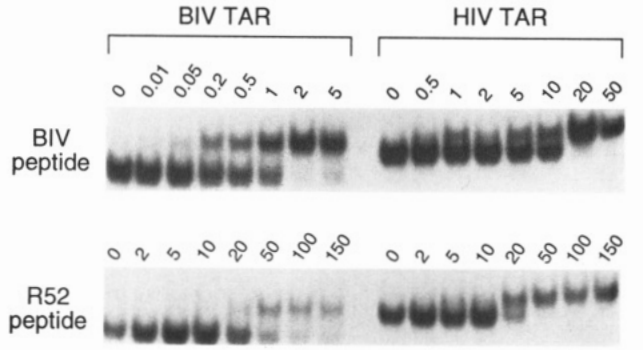

FIGURE 2: Gel shift assays of peptide binding to BIV and HIV TAR RNAs. BIV_{65-81} and R52 (KKKRKKKKK) peptides were incubated with 0.1 nM labeled RNAs at the peptide concentrations indicated (nM), and free RNA and RNA–peptide complexes were separated on polyacrylamide gels.

region that mediates specific binding to the TAR RNA hairpin located at the 5′ end of the viral mRNAs. BIV Tat shares extensive similarity with HIV Tat throughout the essential cysteine-rich and "core" domains and contains a 14 amino acid arginine-rich domain at the same location as the RNA-binding domain of HIV Tat (Figure 1). The 5′ end of the BIV mRNAs contains a potential hairpin structure with similarity to HIV TAR (Figure 1). Thus, it seemed reasonable that the arginine-rich domain of BIV Tat might recognize the BIV hairpin and activate its promoter using a mechanism similar to that of HIV Tat. To examine this possibility, we synthesized a 17 amino acid peptide spanning residues 65–81 of the arginine-rich region of BIV Tat (BIV_{65-81}) and asked whether the peptide would bind specifically to the BIV hairpin. By gel shift analysis, BIV_{65-81} bound to the BIV hairpin at least 20-fold more tightly than to HIV TAR (Figure 2). In contrast, an HIV Tat peptide containing a single arginine residue with eight surrounding lysines (R52; KKKRKKKKK), known to function on HIV TAR (Calnan et al., 1991b), bound to the BIV hairpin with slightly lower affinity than to HIV TAR (Figure 2). Peptides containing the wild-type HIV Tat sequence (RKKRRQRRR) or nine arginines (R9; RRRRRRRRR), also known to function on HIV TAR (Calnan et al., 1991b), also showed little discrimination between the BIV and HIV RNAs (data not shown). Binding titrations performed at several RNA concentrations (Figure 2 shows a titration at 0.1 nM RNA) indicated that BIV_{65-81} binds to the BIV hairpin with an apparent $K_d \approx 0.5$ nM at 4 °C and with 1:1 stoichiometry (data not shown). The shapes of the binding profiles with several RNA variants, particularly those that bound with low affinity (described below), were somewhat different from that of the wild-type RNA, but in all cases apparent K_d values were estimated from the peptide concentrations required to shift 50% of the RNA into the complex. It is unclear why different profiles were observed with some RNAs, although all appear to bind with 1:1 stoichiometries. Because the BIV Tat peptide binds to the BIV hairpin with high affinity and specificity and because the hairpin appears to be required for activation by BIV Tat in the virus (Carpenter et al., 1993), we refer to this RNA element as BIV TAR.

The BIV Tat Arginine-Rich Domain Determines Tat Specificity in Vivo. Previous experiments have shown that BIV Tat efficiently activates the BIV but not the HIV promoter and, conversely, that HIV Tat efficiently activates the HIV but not the BIV promoter (Liu et al., 1992). The specificities of the HIV and SIV Tat proteins also are distinct and are determined by the RNA-binding specificities of their respective arginine-rich RNA-binding domains (Chang & Jeang, 1992; Elangovan et al., 1992; Tao & Frankel, 1993). To compare the in vivo specificities of the RNA-binding regions of BIV and HIV Tat, we constructed a hybrid protein in which the RNA-binding peptide from BIV Tat (residues 65–81) was fused to the activation domain (residues 1–48) of HIV Tat, and a hybrid HIV LTR-CAT reporter in which HIV TAR was replaced by BIV TAR. By placing the RNA-binding domains and RNA sites of BIV and HIV in the same protein and promoter contexts, we could directly compare the RNA-binding specificities of the two proteins, assuming that activation of CAT is proportional to RNA-binding activity.

When assayed on the BIV TAR reporter, the Tat–BIV_{65-81} hybrid protein strongly activated the promoter, whereas the wild-type HIV Tat protein and the HIV R52 protein (Calnan et al., 1991b) were essentially inactive (Figure 3). This supports previous results on the promoter specificity of the intact BIV Tat protein (Liu et al., 1992). When assayed on the HIV TAR reporter, the Tat–BIV_{65-81} hybrid protein showed relatively low activity, whereas the HIV Tat and R52 proteins were highly active (Figure 3). It was expected that the Tat–BIV_{65-81} hybrid protein would function poorly through HIV TAR because, for optimal activity, the single sequence-specific arginine in HIV Tat must be flanked by three basic amino acids on each side and must be located with a fixed spacing relative to the activation domain (Tao & Frankel, 1993). These requirements are not met in the Tat–BIV_{65-81} hybrid protein. Thus, the BIV Tat peptide shows high specificity for BIV TAR in vivo, consistent with the in vitro peptide-binding results.

RNase Mapping and Peptide Footprints. To determine whether the structure of BIV TAR resembled that drawn in Figure 1, we attempted to map the RNA secondary structure using a set of RNases (Figure 4A). Cleavage by the single-strand-specific nucleases PhyM, A, CL3, and T2 indicated that the four-nucleotide loop (CAUU) and the bulged nucleotide U12 were accessible, although not every enzyme cleaved at every expected position (for example, the relatively nonspecific RNase T2 cleaved at only three positions in the loop). Surprisingly, the "bulge" nucleotide U10 was not cleaved by single-strand-specific nucleases (PhyM, A, and

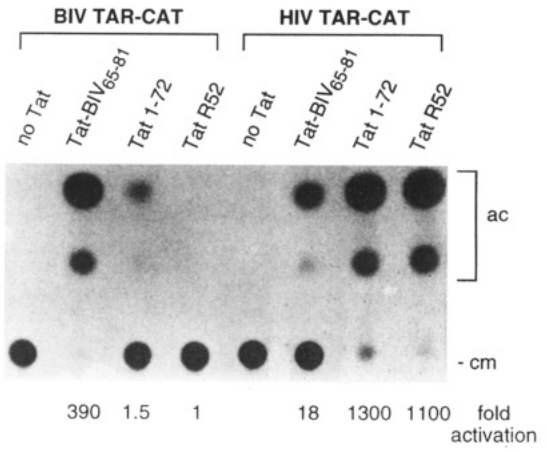

FIGURE 3: Activation of the HIV LTR through the BIV Tat peptide–BIV TAR interaction. HeLa cells were cotransfected with CAT reporter plasmids containing BIV or HIV TAR sites and plasmids expressing an HIV Tat–BIV peptide hybrid protein or HIV Tat proteins. CAT assays were performed 48 h after transfection (Calnan et al., 1991a). Acetylated (ac) and unreacted chloramphenicol (cm) were separated by thin-layer chromatography. For the figure, amounts of extract were assayed that would allow low levels of CAT activity to be seen. However, because some activities were out of the linear range of the assay, assays were repeated with appropriate amounts of extract to quantitate the actual levels of Tat activation (Calnan et al., 1991a).

T2), whereas nucleotides G14 and C23, presumably forming a base pair in the upper stem, were highly accessible to single-strand-specific RNases T1 and CL3. An adjacent nucleotide in the upper stem, C15, also was partially accessible to CL3. Other nucleotides in the upper stem were inaccessible to single-strand-specific nucleases as expected. The double-strand-specific nuclease CV gave an unusual cleavage pattern in which, for example, nucleotides G14 and C15 on the 5′ strand of the upper stem were cleaved but nucleotides G22 and C23 on the opposing 3′ strand were not cleaved. Thus, while the patterns of RNase cleavage (in addition to the mutagenesis experiments described below) are generally consistent with the BIV TAR structure drawn, there are significant differences that are not easily interpreted and may reflect interesting RNA tertiary interactions. It is well-known that RNase cleavage specificities can be influenced markedly by surrounding RNA tertiary structure. For lack of a better structural model, we will refer to the structure as drawn.

RNase cleavage patterns in the presence of the BIV_{65-81} peptide showed several protected bands (Figure 4A), tentatively mapping the peptide-binding site to the bulge and upper stem regions. At high peptide concentrations (corresponding to a peptide:RNA stoichiometry of 1:1), nucleotides C15 and C23 in the upper stem were protected from RNase CL3 cleavage; U12 and U20 were protected from RNase A cleavage; and G9, U10, U24, and C25 were protected from RNase CV cleavage. These protected positions are consistent with chemical interference and mutagenesis data described below. No other obvious changes in nuclease accessibility were observed, suggesting that the RNA structure may not change significantly upon peptide binding. The results of the RNase mapping and protection experiments are summarized in Figure 4B.

Chemical Modification Interference of Peptide Binding. To better define the BIV_{65-81}-binding site and to map nucleotides that might specifically interact with the peptide or be involved in RNA tertiary interactions, we performed chemical modification interference experiments using base- and backbone-specific reagents (Figure 5). Modified RNAs were bound to a BIV_{65-81} peptide affinity column and were eluted with a salt gradient. The elution position of specifically bound RNA was determined using unmodified RNA, and total and bound fractions were cleaved and run on gels to identify positions whose modification interfered with specific binding. Modification of A13 by dimethyl or diethyl pyrocarbonate, which gave identical results, modification of C15, U16, U24, and C25 by hydrazine, and modification of G9, G11, G14, and G22 by dimethyl sulfate strongly interfered with peptide binding. Ethylation of two phosphates, between G9 and U10 and between G22 and C23, also strongly interfered with binding. Ethylation of two additional phosphates, between A21 and G22 and between C23 and U24, weakly interfered with binding. Thus, consistent with the RNase footprints, BIV_{65-81} appears to bind to the bulge and upper stem regions of BIV TAR.

Mutations in BIV TAR Decrease Peptide-Binding Affinity in Vitro and Tat Activation in Vivo. Nucleotides required for specific peptide binding were mapped further by measuring apparent peptide-binding affinities of mutant RNAs. Deleting the U10 bulge nucleotide reduced affinity by almost 20-fold, whereas deleting the U12 bulge nucleotide had only a small effect (Figure 6). Reversing any single GC base pair in the upper stem drastically reduced affinity, by about 200-fold in each case (Figure 6). In contrast, mutation of the loop or replacement of a four-base-pair sequence in the stem with its inverted sequence had little effect on binding (Figure 6B). Thus, the bulge and upper stem regions appear to contain sequence-specific determinants of binding, whereas the loop and lower stem do not, consistent with the RNase protection and chemical interference data.

Several additional mutations were tested to further examine the sequence requirements for binding (Figure 6B). G11·C25 and G14·C23 base pairs were critical for binding and could not be changed to GU pairs. In contrast, the C15·G22 base pair could be changed to a UG pair, but G22 was required. Binding was somewhat sensitive to the identity of the A13·U24 base pair, between the two critical GC pairs, and this position apparently must be paired. In contrast, the U16·A21 base pair at the base of the loop need not be paired. As noted above, the presence of a bulge nucleotide at position 10 is important, but the U can be replaced with other nucleotides. This is consistent with the observation that modification of U10 by hydrazine does not interfere with binding (Figure 5). Thus, it appears that the major sequence determinants for BIV Tat peptide binding are two GC base pairs, one guanine base, and a single bulge nucleotide.

To test whether the apparent peptide-binding affinities measured in vitro accurately reflect RNA binding in vivo, mutant BIV TAR LTR-CAT reporters were constructed and levels of activation were determined using the Tat–BIV_{65-81} hybrid protein (Figure 7). Overall, the in vivo data correlate well with the in vitro data. Substitution of the loop (described below in more detail) or stem sequences, deletion of the U12 bulge, or substitution of the U10 bulge with C had little effect on activity, whereas deletion of the U10 bulge decreased activation about 20-fold. Mutation of the G11·C25 and G14·C23 base pairs (to CG or GU pairs) essentially eliminated activity, whereas mutation of the A13·U24 base pair to UA decreased activity about 15-fold. Substitution of C15·G22 with a UG pair showed the only significant difference between the in vitro and in vivo data; the mutation had a relatively small effect on peptide-binding affinity in vitro but reduced Tat activation about 10-fold in vivo. This mutant RNA has a lowered thermal stability in vitro (L. Chen and A. D. Frankel,

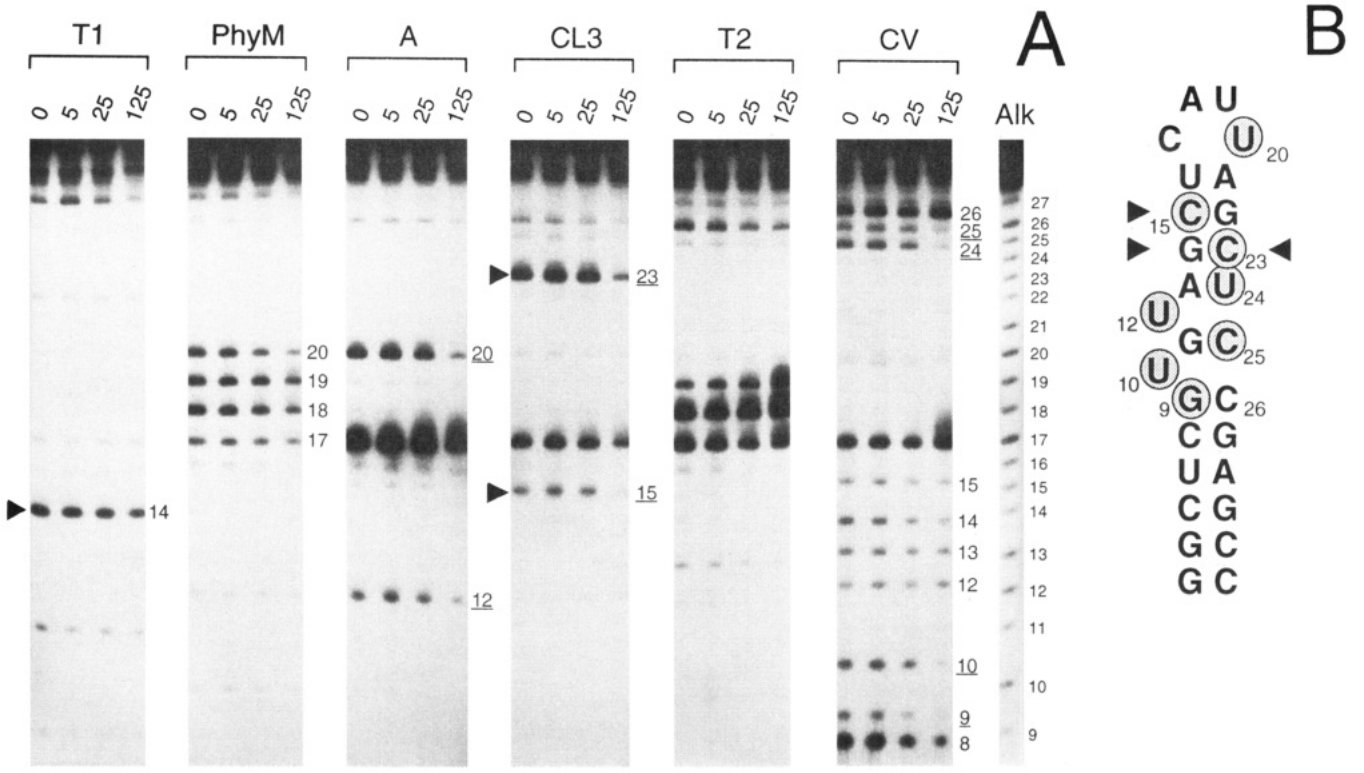

FIGURE 4: RNase mapping of BIV TAR and BIV_{65-81} footprints. (A) In vitro transcribed BIV TAR was labeled with ^{32}P at its 5′ end and digested with RNases (T1, PhyM, A, CL3, CV, and T2) in the absence (0) or presence of 5, 25, or 125 nM BIV_{65-81}. Note that in these experiments the BIV TAR concentration was ~110 nM, well above the apparent K_d for binding, and that the highest peptide concentration corresponds to a peptide:RNA stoichiometry of approximately 1:1 (at which point protected bands are observed). RNases were titrated to cleave the RNA approximately once per molecule. Single-strand-specific nuclease specificities are as follows: RNase T1 cleaves 3′ to guanines, RNase PhyM cleaves 3′ to adenines and uridines, RNase A cleaves 3′ to pyrimidines, RNase CL3 cleaves 3′ to cytidines, and RNase T2 cleaves relatively nonspecifically but with a slight preference 3′ to adenines (Christiansen et al., 1990). RNase CV cleaves double-stranded regions nonspecifically and produces 5′-terminal phosphates. Dark triangles indicate nucleotides accessible to single-strand-specific nucleases although they are expected to be paired: G14 is accessible to RNase T1, and C15 and C23 are accessible to RNase CL3. Positions protected from RNase cleavage at the highest peptide concentration are indicated (underlined numbers). An alkaline digestion ladder (Alk) is included as a control. (B) Summary of the RNase mapping and protection results. Dark triangles correspond to the three nucleotides accessible to single-strand-specific nucleases in the absence of peptide. Circled nucleotides are those protected from cleavage in the presence of peptide.

in preparation), and it is possible that it does not form a stable binding site in vivo. Thus, the in vivo results confirm that the sequence determinants for BIV Tat peptide binding are the G11·C25 and G14·C23 base pairs, G22, and a bulge nucleotide at position 10.

The BIV Tat–TAR Interaction Does Not Appear To Require a Cellular Loop-Binding Protein. In addition to the requirement of the bulge to bind HIV Tat, the six-nucleotide loop of HIV TAR (Figure 1) is required for in vivo activity, probably because a cellular protein is needed to bind to this region. While its precise identity has not yet been established, indirect evidence suggests that the protein may be encoded on human chromosome 12. It has been observed that Tat does not function efficiently in rodent cells unless human chromosome 12 is present (Hart et al., 1989; Newstein et al., 1990). However if Tat is delivered to the LTR by a heterologous RNA-binding protein, chromosome 12 is not required (Alonso et al., 1992; Madore & Cullen, 1993), suggesting that chromosome 12 does not encode a protein needed for Tat activation per se. Rather, because the TAR loop is not present in the context of these heterologous systems, it seems plausible that chromosome 12 provides a loop-binding protein that helps stabilize the relatively weak HIV Tat–TAR interaction. Consistent with this view is the finding that mutations in the loop do not decrease the level of TAT activation in rodent cells in the absence of chromosome 12 (Hart et al., 1993).

In contrast to HIV Tat, BIV Tat does not appear to require a loop-binding protein to stabilize binding to BIV TAR. As described above, mutation of the BIV TAR loop (from CAUU to UGCC) did not affect peptide-binding affinity in vitro or Tat activity in vivo. Twelve additional loop mutants were constructed containing single nucleotide substitutions; these all had in vitro BIV_{65-81}-binding affinities similar to wild-type BIV TAR (except the G20 mutant, which formed RNA dimers; data not shown). These data are consistent with a previously described loop mutant (Carpenter et al., 1993). To examine further the loop requirements in vivo, we asked whether HIV Tat, delivered to the HIV LTR via the BIV peptide targeted to BIV TAR, would function in rodent cells. Indeed, the hybrid protein activates the promoter efficiently in mouse cells, whereas HIV Tat delivered via HIV TAR activates relatively poorly (Figure 8). Taken together, the data suggest that the BIV TAR loop binds neither BIV Tat nor a cellular factor and that the direct interaction between BIV Tat and BIV TAR is sufficient to mediate Tat activation in vivo.

DISCUSSION

We have shown that a 17 amino acid arginine-rich peptide from BIV Tat (BIV_{65-81}) binds to the BIV TAR hairpin with high specificity and affinity (apparent $K_d \approx 0.5$ nM). While the sequences of the HIV and BIV TAR RNAs are similar, the features recognized by their respective proteins are distinct (Figure 9). In HIV TAR, a single arginine-binding site is formed by a guanine base and two phosphates at a bulge; the conformation of the site appears to be stabilized by a base triple between the 5′-most uridine in the bulge and an AU base pair above the bulge (Puglisi et al., 1992, 1993). In BIV

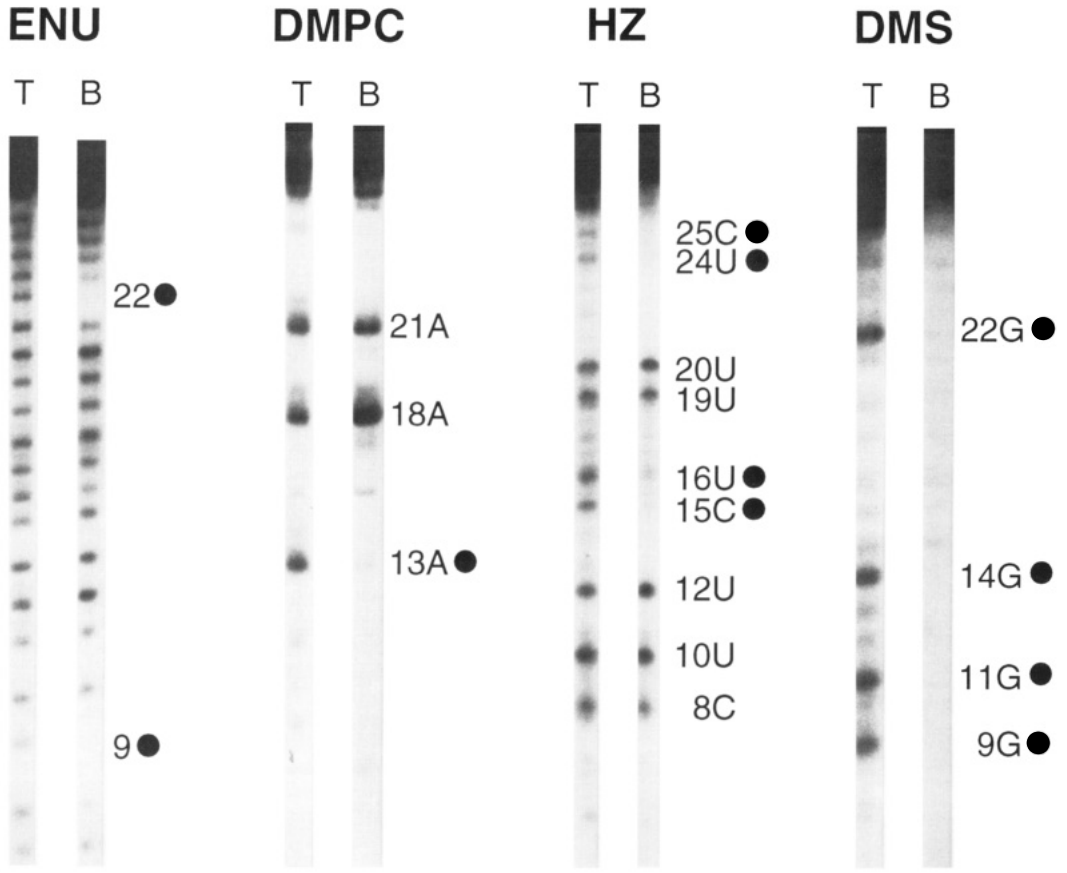

FIGURE 5: Chemical modification interference of BIV_{65-81} binding to BIV TAR. In vitro transcribed BIV TAR was labeled with ^{32}P at its 5′ end and modified with ethylnitrosourea (ENU), dimethyl pyrocarbonate (DMPC), hydrazine (HZ), or dimethyl sulfate (DMS) under conditions that modify less than one site per molecule. Modified RNAs were bound to a BIV_{65-81} peptide affinity column, eluted with a salt gradient, and cleaved. Total (T) and specifically bound (B) RNAs were compared on polyacrylamide gels. Positions whose modification interferes with specific binding are indicated by dark circles.

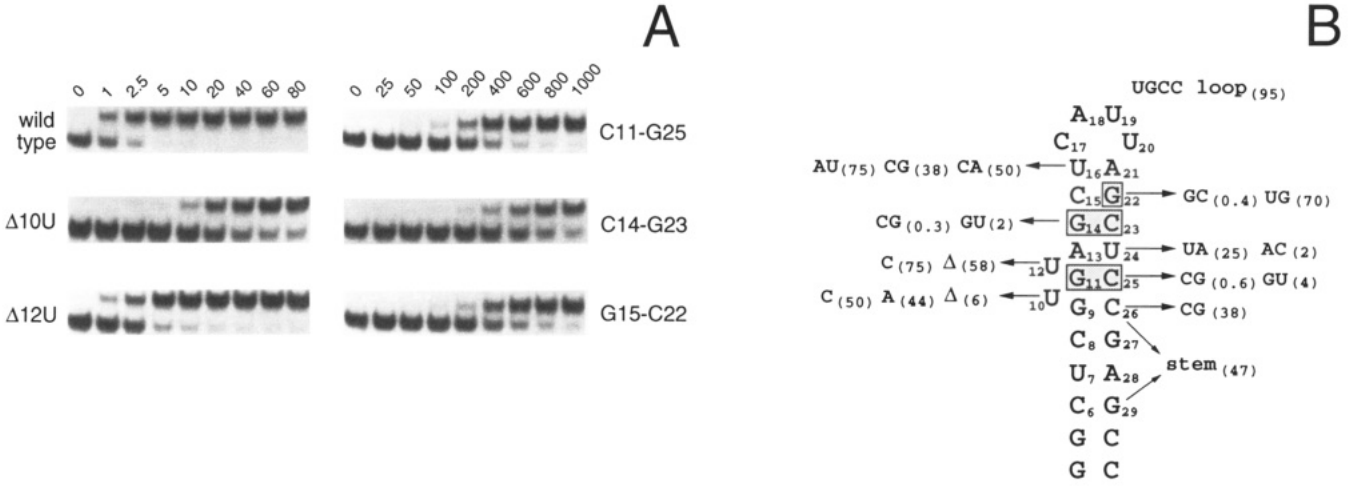

FIGURE 6: Effects of BIV TAR mutations on BIV_{65-81} binding in vitro. (A) Gel shift assays with wild-type BIV TAR and several mutants. Binding reaction mixtures contained labeled RNA, 25 μg/mL competitor tRNA, and BIV_{65-81} at the concentrations indicated (nM). (B) Summary of peptide binding to BIV TAR mutants. Numbers in parentheses indicate percent binding relative to wild-type BIV TAR [100 K_d(wt)/K_d(mut)]. Apparent K_d values represent peptide concentrations at which 50% of the RNA is shifted into the complex. The loop mutant contains a substitution of nucleotides 17–20 (CAUU to UGCC). The stem mutant contains a substitution of four base pairs (C6·G29, U7·A28, C8·G27, and G9·C26 to G6·C29, A7·U28, G8·C27, and C9·G26) that maintains the nucleotide composition and base-pairing stability of the lower stem.

TAR, it appears that three guanines (one adjacent to a single-nucleotide bulge and two near the ends of a stem) and two phosphates (one adjacent to the bulge and the other in a stem) are particularly important for binding. It is not yet known which amino acids in the BIV Tat peptide contact these and/or other RNA groups or whether additional RNA–RNA tertiary interactions occur; however, RNase mapping experiments suggest that the RNA may form an unusual structure: at least one GC base pair in the middle of an apparent stem is highly accessible to nuclease cleavage. It is interesting that the TAR structure of one SIV isolate (MND) has characteristics of both HIV and BIV; it has the same bulge structure as BIV but an altered stem sequence, and it has a loop sequence similar to that of HIV (Berkhout, 1992).

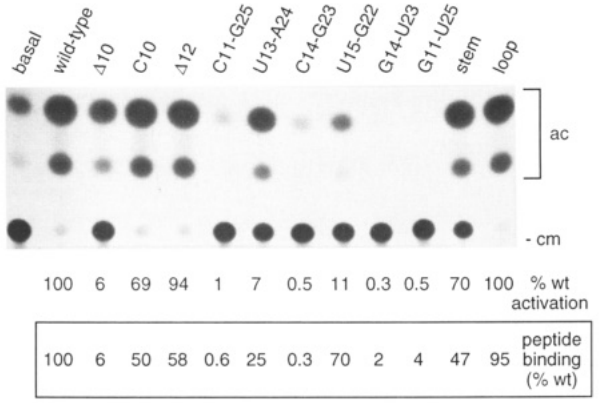

FIGURE 7: Effect of BIV TAR mutations on BIV_{65-81}-mediated activation in vivo. HeLa cells were cotransfected with CAT reporter plasmids containing wild-type BIV TAR or BIV TAR mutants and a plasmid expressing the Tat–BIV_{65-81} hybrid protein. As described in Figure 3, amounts of extract were assayed that would allow low levels of CAT activity to be seen. Basal activities (in the absence of the hybrid protein) were determined for each mutant reporter plasmid (data not shown) to calculate levels of activation. Thus, while the activity of the U13·A24 mutant, for example, appears higher than that of the U15·G22 mutant, it actually is lower when adjusted for differences in basal activity. For comparison, levels of activation were normalized to wild-type BIV TAR, and in vitro apparent peptide-binding affinities for each mutant (from Figure 6B) are shown beneath them (boxed).

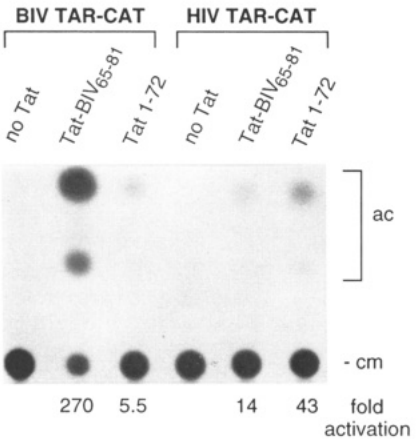

FIGURE 8: Activation mediated by the BIV_{65-81}–BIV TAR interaction is efficient in rodent cells. Mouse LTk⁻ cells were cotransfected with CAT reporter plasmids containing BIV or HIV TAR sites and plasmids expressing the Tat–BIV_{65-81} hybrid protein or wild-type HIV Tat. CAT assays were performed as in Figure 3.

The BIV Tat–TAR interaction is the third case in which a short basic peptide has been found to bind specifically to an RNA hairpin. The similarities, and the rather striking differences, seen in these simple systems have provided some new perspectives on RNA–protein recognition. In HIV Tat, a single arginine residue, surrounded by at least three basic amino acids on each side, is required for sequence-specific recognition of HIV TAR (Calnan et al., 1991b). In its unbound form, the peptide appears to be unstructured, even in the context of the intact protein (Calnan et al., 1991a,b). In HIV Rev, a 17 amino acid peptide binds specifically to the RRE hairpin but only when in an α-helical conformation (Tan et al., 1993). The Rev–RRE interaction requires six amino acids—four arginines, one threonine, and one asparagine—for sequence-specific recognition (Tan et al., 1993). In both cases, the RNAs undergo conformational changes upon peptide binding (Puglisi et al., 1992; Tan & Frankel, 1992; Tan et al., 1993).

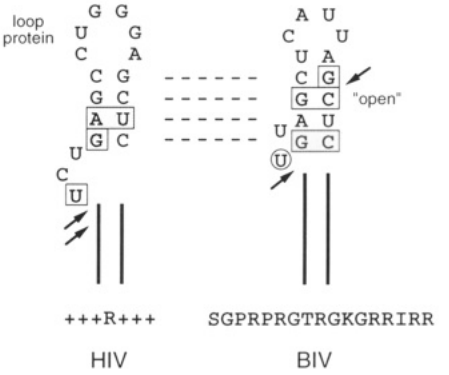

FIGURE 9: Comparison of HIV and BIV Tat–TAR recognition. Nucleotides important for RNA recognition by their respective peptides are boxed, and positions of phosphates whose modification interferes with binding are indicated by arrows. For BIV TAR, the important nucleotides are taken from the mutagenesis results (Figure 6B), and the circled U indicates that a bulge nucleotide is important but its identity is not. Two more weakly interfering phosphates in BIV TAR (not shown) are described in the text. RNase footprinting and chemical modification interference experiments (Figures 4 and 5) are consistent with the mutagenesis results; however, the interference experiments identified several additional nucleotides whose modification interferes with binding. It is possible that some of these modifications cause steric hindrance or change the RNA structure rather than indicate RNA–protein contacts or RNA tertiary interactions. A putative GC base pair in the middle of the upper stem of BIV TAR is accessible to nucleases ("open"). A cellular loop-binding protein appears to be necessary for Tat activation in the HIV but not the BIV system.

The BIV Tat–TAR interaction shows both similarities to and differences from the HIV Tat–TAR and Rev–RRE examples. Circular dichroism experiments suggest that BIV_{65-81}, like HIV Tat peptides, is unstructured in the absence of RNA (L. Chen and A. D. Frankel, in preparation). The unstructured nature of the peptide is supported by its relatively high proline and glycine content. Unlike HIV Tat, several amino acids, including at least two arginines and one threonine, are needed for sequence-specific binding by BIV_{65-81} (L. Chen and A. D. Frankel, in preparation). Given the importance of guanines and phosphates in the BIV-binding site and arginines in the BIV peptide, it seems plausible that some part of the interaction may resemble the arginine–guanine–phosphate interaction proposed for HIV TAR (Puglisi et al., 1992). Similar contacts also may occur in the Rev peptide–RRE interaction (Tan et al., 1993). The importance of a threonine in both the BIV and Rev peptides may suggest additional similarities. RNase mapping of BIV TAR (Figure 4) and circular dichroism experiments (L. Chen and A. D. Frankel, in preparation) suggest that, unlike HIV TAR and RRE RNAs, BIV TAR may not change its conformation significantly upon peptide binding. The unusual structure of BIV TAR appears to be stable in the absence of peptide and may provide a relatively fixed binding surface for amino acids in BIV_{65-81}. More detailed structural studies will be needed to determine the precise structure of BIV TAR, the nature of any undetected conformational changes, and the amino acid–RNA contacts. Nevertheless, it already seems obvious that no simple recognition code will be found for RNA–protein recognition, even in apparently related systems, and that structural comparisons between related and unrelated recognition motifs will be needed to better understand the contributions to sequence specificity.

The BIV Tat–TAR interaction is further distinct from the HIV Tat–TAR interaction in that BIV does not appear to require additional cellular proteins to help stabilize RNA binding in vivo. The affinity and specificity of the BIV

interaction are significantly higher than those of the HIV interaction, and additional factors probably are unnecessary. Thus, not only have the two viruses evolved different recognition elements in their Tat RNA-binding domains and TAR RNA-binding sites, but they have achieved different dependencies on their host environments. It is tempting to speculate that cellular proteins may be needed for HIV Tat-mediated activation to gain additional levels of cell-type-specific or temporal control of viral expression during HIV infection, perhaps to help maintain the virus in a latent or attentuated state. Little is known currently about the target cells for BIV infection, the differences in regulatory factors between bovine cell types, and the precise mechanism of BIV Tat activation. Further comparisons between the bovine and human systems may reveal interesting differences in viral regulatory mechanisms that may relate to differences in viral pathogenicity.

ACKNOWLEDGMENT

We thank Kazuo Harada and Derek Hudson for peptide synthesis, David King for mass spectrometry, Chris Seibel for helpful suggestions, and Hua Yang for technical assistance. We thank members of the laboratory for helpful discussions and Keith Yamamoto, Hiten Madhani, Mark Feinberg, Raul Andino, and John Young for comments on the manuscript.

REFERENCES

Alonso, A., Derse, D., & Peterlin, B. M. (1992) *J. Virol. 66*, 4617–4621.
Berkhout, B. (1992) *Nucleic Acids Res. 20*, 27–31.
Calnan, B. J., Biancalana, S., Hudson, D., & Frankel, A. D. (1991a) *Genes Dev. 5*, 201–210.
Calnan, B. J., Tidor, B., Biancalana, S., Hudson, D., & Frankel, A. D. (1991b) *Science 252*, 1167–1171.
Carpenter, S., Nadin-Davis, S. A., Wannemuehler, Y., & Roth, J. A. (1993) *J. Virol. 67*, 4399–4403.
Cavarelli, J., Rees, B., Ruff, M., Thierry, J. C., & Moras, D. (1993) *Nature 362*, 181–184.
Chang, Y. N., & Jeang, K. T. (1992) *Nucleic Acids Res. 20*, 5465–5472.
Christiansen, J., Egebjerg, J., Larsen, N., & Garrett, R. A. (1990) in *Ribosomes and Protein Synthesis* (Spedding, G., Ed.) pp 229–252, Oxford University Press, Oxford.
Elangovan, B., Subramanian, T., & Chinnadurai, G. (1992) *J. Virol. 66*, 2031–2036.
Frankel, A. D. (1992) *Protein Sci. 1*, 1539–1542.
Garvey, K. J., Oberste, M. S., Elser, J. E., Braun, M. J., & Gonda, M. A. (1990) *Virology 175*, 391–409.
Gonda, M. A. (1992) *AIDS 6*, 759–776.
Hart, C. E., Ou, C. Y., Galphin, J. C., Moore, J., Bacheler, L. T., Wasmuth, J. J., Petteway, S. R., Jr., & Schochetman, G. (1989) *Science 246*, 488–491.
Hart, C. E., Galphin, J. C., Westhafer, M. A., & Schochetman, G. (1993) *J. Virol. 67*, 5020–5024.
Kjems, J., Calnan, B. J., Frankel, A. D., & Sharp, P. A. (1992) *EMBO J. 11*, 1119–1129.
Lazinski, D., Grzadzielska, E., & Das, A. (1989) *Cell 59*, 207–218.
Liu, Z. Q., Sheridan, D., & Wood, C. (1992) *J. Virol. 66*, 5137–5140.
Madore, S. J., & Cullen, B. R. (1993) *J. Virol. 67*, 3703–3711.
Milligan, J. F., & Uhlenbeck, O. C. (1989) *Methods Enzymol. 180*, 51–62.
Newstein, M., Stanbridge, E. J., Casey, G., & Shank, P. R. (1990) *J. Virol. 64*, 4565–4567.
Pallansch, L. A., Lackman-Smith, C. S., & Gonda, M. A. (1992) *J. Virol. 66*, 2647–2652.
Peattie, D. A. (1979) *Proc. Natl. Acad. Sci. U.S.A. 76*, 1760–1764.
Puglisi, J. D., Tan, R., Calnan, B. J., Frankel, A. D., & Williamson, J. R. (1992) *Science 257*, 76–80.
Puglisi, J. D., Chen, L., Frankel, A. D., & Williamson, J. R. (1993) *Proc. Natl. Acad. Sci. U.S.A. 90*, 3680–3684.
Rould, M. A., Perona, J. J., Soll, D., & Steitz, T. A. (1989) *Science 246*, 1135–1142.
Rould, M. A., Perona, J. J., & Steitz, T. A. (1991) *Nature 352*, 213–218.
Ruff, M., Krishnaswamy, S., Boeglin, M., Poterszman, A., Mitschler, A., Podjarny, A., Rees, B., Thierry, J. C., & Moras, D. (1991) *Science 252*, 1682–1689.
Tan, R., & Frankel, A. D. (1992) *Biochemistry 31*, 10288–10294.
Tan, R., Chen, L., Buettner, J. A., Hudson, D., & Frankel, A. D. (1993) *Cell 73*, 1031–1040.
Tao, J., & Frankel, A. D. (1992) *Proc. Natl. Acad. Sci. U.S.A. 89*, 2723–2726.
Tao, J., & Frankel, A. D. (1993) *Proc. Natl. Acad. Sci. U.S.A. 90*, 1571–1575.
Weeks, K. M., Ampe, C., Schultz, S. C., Steitz, T. A., & Crothers, D. M. (1990) *Science 249*, 1281–1285.